Survival probabilities and first-passage distributions of self-propelled particles in spherical cavities

Binny J. Cherayil*

Department of Inorganic and Physical Chemistry, Indian Institute of Science, Bangalore 560012, Karnataka, India

(Received 13 March 2023; accepted 5 November 2023; published 20 November 2023)

A model of self-propelled motion in a closed compartment containing simple or complex fluids is formulated in this paper in terms of the dynamics of a point particle moving in a spherical cavity under the action of random thermal forces and exponentially correlated noise. The particle's time evolution is governed by a generalized Langevin equation (GLE) in which the memory function, connected to the thermal forces by a fluctuation-dissipation relation, is described by Jeffrey's model of viscoelasticity (which reduces to a model of ordinary viscous dynamics in a suitable limit). The GLE is transformed exactly to a Fokker-Planck equation that in spherical polar coordinates is in turn found to admit of an exact solution for the particle's probability density function under absorbing boundary conditions at the surface of the sphere. The solution is used to derive an expression (that is also exact) for the survival probability of the particle in the sphere, starting from its center, which is then used to calculate the distribution of the particle's first-passage times to the boundary. The behavior of these quantities is investigated as a function of the Péclet number and the persistence time of the athermal forces, providing insight into the effects of nonequilibrium fluctuations on confined particle motion in three dimensions.

DOI: 10.1103/PhysRevE.108.054607

I. INTRODUCTION

The motion of particles through living cells is one of several stochastic processes with important implications for the cells' biochemical functioning [1]. Viral infection—whereby an endocytosed virus particle makes its way from a cell's periphery to the interior of its nucleus—represents an especially consequential outcome of the interplay between particle motion and cellular viability [2–5]. The process often involves a combination of passive diffusion, driven by thermal fluctuations in the surroundings, and active transport, in which microtubules, motor proteins, or other energy-transducing molecules are recruited to produce directed movement.

Efforts to uncover the microscopic roots of such processes have been wide ranging, and have proceeded along many different lines of experimental, numerical, and analytical enquiry, including studying self-propelled diffusion through complex heterogeneous media [6–18], developing models of free or confined active Brownian transport [19–28], and analyzing random particle entry into or egress from small patches embedded in aqueous compartments [29–37]. The last set of approaches, which broadly address what are often referred to as narrow escape problems, is especially relevant to the study of viral and intracellular trafficking. But the treatment of such problems appears to have so far been limited to situations in which particle dynamics takes place in purely Newtonian liquids, or under conditions of reduced dimensionality. As far as can be ascertained, the more realistic situation of escape from or diffusion through three-dimensional regions that enclose the kind of non-Newtonian liquids that characterize cellular interiors has yet to be fully explored. In an effort to enlarge our understanding of such situations, a study is undertaken in this paper of a model of active particle transport in a spherical cavity containing a viscous or a viscoelastic medium. (The former is a special case of the latter.) The model is formulated in terms of the overdamped motion of a spherically confined point particle that experiences forces from both thermal fluctuations (which satisfy a fluctuation-dissipation theorem) and exponentially damped external noise (which does not). The particle's dynamics are therefore those of a thermally driven active Ornstein-Uhlenbeck particle (AOUP) [38]. The effects of viscoelasticity are incorporated into the model through a memory function in the generalized Langevin equation (GLE) that is assumed to govern the particle's time evolution [39]. The equation is used to calculate—via an exact transformation to an equivalent Fokker-Planck equation in spherical polar coordinates—the survival probability of the particle in the sphere when it starts off from the sphere's center and is absorbed at its boundary. The survival probability, in turn, is used to calculate the distribution of the particle's first-passage times to the boundary.

First-passage times convey information about the likely duration of stochastic events that terminate on attaining a critical threshold [40], and in the case of spatially confined self-propelled particles whose motion ceases on arriving at a boundary, they are also measures of escape or capture times [41]. The calculations in this paper complement recent work by Di Trapani *et al.* [42] on the dynamics of active Brownian particles (ABPs) in circular disks with absorbing boundaries, which also employs a Fokker-Planck formalism to obtain survival probabilities and first-passage distributions. In relation to that report, the work discussed here is significant in the following respects: (i) It is more easily implemented,

*cherayil@iisc.ac.in

since AOUP dynamics do not explicitly consider the particle's directional fluctuations [38], which in the case of ABPs are coupled to position coordinates [43], and which therefore necessitate the use of the kind of elaborate matrix methods employed in Ref. [42]. (ii) It yields exact results (which, for our chosen system, bear strong qualitative similarities to the findings in that reference). (iii) It is more directly relevant to stochastic biological phenomena, being formulated in three dimensions and applying to viscoelastic media. (iv) It allows for the relatively straightforward incorporation of additional realistic details into the model (such as external potentials and power law correlations of the active fluctuations) that may be important in the design and fabrication of synthetic microswimmers with well-defined dynamical properties.

The paper is organized as follows. The next section reviews the generalized Langevin equation that governs the particle's time evolution in three dimensions (in Cartesian space) under the action of random thermal and athermal forces. Section III recasts this equation as a Fokker-Planck equation in spherical polar coordinates, and then solves it under an absorbing boundary condition at the surface of the sphere that is imagined to confine the particle. The solution is used in Sec. IV to calculate—analytically—the survival probability of the particle in the sphere, and from there the distribution of the particle's first-passage times to the boundary. Section V presents the results of these calculations, and discusses their implications.

II. GLE MODEL OF PARTICLE DYNAMICS

The self-propelled particle in this study is assumed to evolve in time in the absence of an external potential according to the following generalized Langevin equation [39]:

$$\zeta \int_0^t dt' K(t-t')\dot{x}_i(t') = \theta_i(t) + \xi_i(t), \;\; i = 1, 2, 3. \tag{1}$$

Here, $\mathbf{x}(t)$ is the position of the particle in three dimensions at time t, with $x_i(t)$ its Cartesian component along the ith axis, ζ is the particle's friction coefficient, and $\theta(t)$ and $\xi(t)$ are Gaussian random variables, the first representing thermal fluctuations from the surrounding medium, and the second representing athermal forces originating either in the particle's own internal energy or in an independent external source [15]. The variable $\boldsymbol{\theta}(t)$ is defined completely by the moments $\langle\theta_i(t)\rangle = 0$ and $\langle\theta_i(t)\theta_j(t')\rangle = \zeta k_B T \delta_{i,j} K(|t-t'|)$, where k_B is Boltzmann's constant, T is the temperature, and $K(t)$ is a memory function (to be specified later), while $\boldsymbol{\xi}(t)$ [which is independent of $\boldsymbol{\theta}(t)$] is defined by the moments $\langle\xi_i(t)\rangle = 0$ and $\langle\xi_i(t)\xi_j(t')\rangle = \varepsilon\delta_{i,j}M(|t-t'|)$, where $\sqrt{\varepsilon}$ is a measure of the strength of the self-driving force, and $M(t)$ is defined as $M(t) = e^{-t/\tau}$, with τ a decay constant. In this model of $\boldsymbol{\xi}(t)$, the athermal force has the same statistical correlations as Ornstein-Uhlenbeck noise.

III. EQUIVALENT FOKKER-PLANCK DESCRIPTION

The calculation of survival probabilities and first-passage distributions from Eq. (1) proceeds by converting the equation to an equivalent Fokker-Planck equation for the probability density, $P(\mathbf{x}, t)$, of finding the particle at the point $\mathbf{x}$ at time t, and then solving this equation under appropriate boundary conditions. The conversion is effected by using Laplace transforms and their inverses to first rewrite Eq. (1) in the form [44,45]

$$\dot{x}_i(t) = \frac{1}{\zeta}[\bar{\theta}_i(t) + \bar{\xi}_i(t)], \tag{2a}$$

where

$$\bar{\theta}_i(t) \equiv \frac{d}{dt}\int_0^t dt' \phi(t-t')\theta_i(t'), \tag{2b}$$

$$\bar{\xi}_i(t) \equiv \frac{d}{dt}\int_0^t dt' \phi(t-t')\xi_i(t'), \tag{2c}$$

and $\phi(t)$ is the Laplace inverse of the function $\hat{\phi}(s) = 1/[s\hat{K}(s)]$, the Laplace transform $\hat{f}(s)$ of a function $f(t)$ being defined through the operation $\mathcal{L}_s f(t) \equiv \hat{f}(s) = \int_0^\infty dt e^{-st} f(t)$.

Then, from the definition

$$P(\mathbf{x}, t) = \left\langle \prod_{i=1}^{3} \delta[x_i - x_i(t)] \right\rangle, \tag{3}$$

where the angular brackets denote an average with respect to different realizations of the noise, an equation for $\partial P(\mathbf{x}, t)/\partial t$ is derived by differentiating Eq. (3) with respect to t, invoking the derivative property of the delta function $[\partial\delta(x-y)/\partial x = -\partial\delta(x-y)/\partial y]$, and substituting the relation for $\dot{x}_i(t)$ from Eq. (2a); the result is

$$\frac{\partial P(\mathbf{x}, t)}{\partial t} = -\frac{1}{\zeta}\sum_{j=1}^{3}\frac{\partial}{\partial x_j}\left\langle \prod_{i=1}^{3}\delta[x_i - x_i(t)][\bar{\theta}_j(t) + \bar{\xi}_j(t)]\right\rangle. \tag{4}$$

The averages $T_1 \equiv \langle\prod_{i=i}^{3}\delta[x_i - x_i(t)]\bar{\theta}_j(t)\rangle$ and $T_2 \equiv \langle\prod_{i=i}^{3}\delta[x_i - x_i(t)]\bar{\xi}_j(t)\rangle$ that appear in Eq. (4) can each be reduced to simpler forms using Novikov's theorem [46], which when applied to T_1 yields

$$T_1 = \int_0^t dt' \langle\bar{\theta}_j(t)\bar{\theta}_j(t')\rangle\left\langle \frac{\delta}{\delta\bar{\theta}_j(t')}\prod_{i=1}^{3}\delta[x_i - x_i(t)]\right\rangle. \tag{5}$$

On applying the chain rule of differentiation to the second term in angular brackets, along with the derivative property of the delta function, Eq. (5) becomes

$$T_1 = -\sum_{k=1}^{3}\frac{\partial}{\partial x_k}\int_0^t dt' \langle\bar{\theta}_j(t)\bar{\theta}_j(t')\rangle\left\langle \prod_{i=1}^{3}\delta[x_i - x_i(t)]\frac{\delta x_k(t)}{\delta\bar{\theta}_j(t')}\right\rangle. \tag{6}$$

From Eq. (2a), it follows that

$$\frac{d}{dt}\frac{\delta x_k(t)}{\delta\bar{\theta}_j(t')} = \frac{1}{\zeta}\delta_{j,k}\delta(t-t'),$$

and hence that

$$\frac{\delta x_k(t)}{\delta\bar{\theta}_j(t')} = \frac{1}{\zeta}\delta_{j,k}H(t-t'), \tag{7}$$

where $H(t-t')$ is the Heaviside step function. The substitution of Eq. (7) into Eq. (6) leads to the following result:

$$T_1 = -\frac{1}{\zeta}\frac{\partial}{\partial x_j}\int_0^t dt' \langle\bar{\theta}_j(t)\bar{\theta}_j(t')\rangle P(\mathbf{x}, t). \tag{8}$$

In the same way, it can be shown that

$$T_2 = -\frac{1}{\zeta}\frac{\partial}{\partial x_j}\int_0^t dt' \langle \bar{\xi}_j(t)\bar{\xi}_j(t')\rangle P(\mathbf{x},t). \tag{9}$$

When the expressions for T_1 and T_2 are substituted into Eq. (4), the evolution equation for $P(\mathbf{x},t)$ assumes the form

$$\frac{\partial P(\mathbf{x},t)}{\partial t} = \frac{1}{\zeta^2}\sum_{j=1}^{3} I_1(t)\frac{\partial^2}{\partial x_j^2}P(\mathbf{x},t) + \frac{1}{\zeta^2}\sum_{j=1}^{3} I_2(t)\frac{\partial^2}{\partial x_j^2}P(\mathbf{x},t), \tag{10}$$

where $I_1(t) \equiv \int_0^t dt' \langle \bar{\theta}_j(t)\bar{\theta}_j(t')\rangle$ and $I_2(t) \equiv \int_0^t dt' \langle \bar{\xi}_j(t)\bar{\xi}_j(t')\rangle$. These two functions can be evaluated following well-known methods discussed extensively elsewhere [44,45], but for completeness a few pertinent details of the relevant calculations are sketched below, using the case of $I_1(t)$ as an illustration. Its evaluation begins by substituting the expression for $\bar{\theta}_j(t)$ from Eq. (2b) into its definition, which leads to

$$I_1(t) = \left\langle \left(\frac{d}{dt}\int_0^t dt_1 \phi(t-t_1)\theta_j(t_1)\right)\int_0^t dt' \frac{d}{dt'}\int_0^{t'} dt_2 \phi(t'-t_2)\theta_j(t_2)\right\rangle = \left\langle \left(\frac{d}{dt}\int_0^t dt_1 \phi(t-t_1)\theta_j(t_1)\right)\int_0^t dt_2 \phi(t-t_2)\theta_j(t_2)\right\rangle. \tag{11a}$$

The product rule of differentiation in the form $u\frac{d}{dt}v = \frac{d}{dt}uv - v\frac{d}{dt}u$ is now applied to Eq. (11a), with the identifications $u = \int_0^t dt_2 \phi(t-t_2)\theta_j(t_2)$ and $v = u = \int_0^t dt_1 \phi(t-t_1)\theta_j(t_1)$, such that $u\frac{d}{dt}v = \frac{1}{2}\frac{d}{dt}uv$, and hence

$$\begin{aligned} I_1(t) &= \frac{1}{2}\frac{d}{dt}\int_0^t dt_1 \int_0^t dt_2 \phi(t-t_1)\phi(t-t_2)\langle \theta_j(t_1)\theta_j(t_2)\rangle \\ &= \frac{1}{2}\frac{d}{dt}\lim_{t'\to t}\int_0^t dt_1 \int_0^{t'} dt_2 \phi(t-t_1)\phi(t'-t_2)\langle \theta_j(t_1)\theta_j(t_2)\rangle. \end{aligned} \tag{11b}$$

The convolution property of Laplace transforms now allows Eq. (11b) to be written as

$$I_1(t) = \frac{1}{2}\frac{d}{dt}\lim_{t'\to t}\mathcal{L}_s^{-1}\mathcal{L}_{s'}^{-1}\hat{\phi}(s)\hat{\phi}(s')\langle \hat{\theta}_j(s)\hat{\theta}_j(s')\rangle, \tag{12}$$

where $\mathcal{L}_s^{-1}$ and $\mathcal{L}_{s'}^{-1}$ are, respectively, the inverse Laplace transforms with respect to the variables s and s', which are conjugate, respectively, to the variables t and t'. The substitution of the definition $\hat{\phi}(s) = 1/[s\hat{K}(s)]$ into Eq. (12), along with the double Laplace transform of the correlation function $\langle \theta_j(t)\theta_j(t')\rangle = \zeta k_B T K(|t-t'|)$, then produces

$$I_1(t) = \frac{1}{2}\zeta k_B T \frac{d}{dt}\lim_{t'\to t}\mathcal{L}_s^{-1}\mathcal{L}_{s'}^{-1}\left[\frac{1}{ss'(s+s')}\left\{\frac{1}{\hat{K}(s')} + \frac{1}{\hat{K}(s)}\right\}\right]. \tag{13}$$

Along the same lines,

$$I_2(t) = \frac{1}{2}\varepsilon\frac{d}{dt}\lim_{t'\to t}\mathcal{L}_s^{-1}\mathcal{L}_{s'}^{-1}\left[\frac{1}{ss'(s+s')\hat{K}(s)\hat{K}(s')}\left\{\frac{1}{(s+\tau^{-1})} + \frac{1}{(s'+\tau^{-1})}\right\}\right]. \tag{14}$$

Once a definite form of the memory function $K(t)$ is specified, the functions $I_1(t)$ and $I_2(t)$ can be determined (in principle.) For the present calculations, $K(t)$ is taken to correspond to the Jeffrey's model of viscoelasticity used by Ferrer *et al.* [47] to fit the results of their experiments on the barrier crossing dynamics of optically trapped colloidal silica particles to the predictions of Kramers' theory. In this model (a variant of which was used by Ginot *et al.* [48]—under the name Maxwell model—in simulations of related barrier crossing experiments), $K(t)$ is given by

$$K(t) = \frac{1}{\zeta}\left[2\gamma_\infty \delta(t) + \frac{\gamma_s - \gamma_\infty}{\tau_s}e^{-t/\tau_s}\right], \tag{15}$$

where τ_s is the relaxation time of the fluid, and γ_∞ and γ_s are friction coefficients related, respectively, to the solvent viscosity and zero-shear viscosity, η_∞ and η_s, by $\gamma_\infty = 3\pi d_p \eta_\infty$ and $\gamma_s = 3\pi d_p \eta_s$, with d_p the diameter of the particle. From the results reported by Ferrer *et al.* [47], the empirical parameters in Eq. (15) assume the values $\tau_s = 1.148$ s, $\gamma_\infty = 3.732 \times 10^{-8}$ N m^{-1} s, , and $\gamma_s = 3.919 \times 10^{-7}$ N m^{-1} s. These values are used in the subsequent calculations as an illustration of the kind of results that might be obtained for a reasonably realistic description of an actual system [49].

With $K(t)$ defined by Eq. (15), $I_1(t)$ and $I_2(t)$ are easily found in closed form from Eqs. (13) and (14), and when these expressions are then substituted into Eq. (10), the following Fokker-Planck equation is obtained:

$$\frac{\partial P(\mathbf{x},t)}{\partial t} = D_1(t)\nabla_{\mathbf{x}}^2 P(\mathbf{x},t) + D_2(t)\nabla_{\mathbf{x}}^2 P(\mathbf{x},t), \tag{16a}$$

where

$$D_1(t) = \frac{k_B T}{\gamma_s}\left[1 + \frac{(\gamma_s - \gamma_\infty)}{\gamma_\infty} e^{-\gamma_s t/\gamma_\infty \tau_s}\right], \tag{16b}$$

and

$$D_2(t) = \frac{\varepsilon \tau}{\gamma_s^2}\left[1 + \frac{(\gamma_s - \gamma_\infty)}{\gamma_\infty} e^{-\gamma_s t/\gamma_\infty \tau_s}\right]\left[1 + \frac{\tau_s(\gamma_\infty - \gamma_s)}{\gamma_s \tau - \gamma_\infty \tau_s} e^{-\gamma_s t/\gamma_\infty \tau_s} - \frac{\gamma_s(\tau - \tau_s)}{\gamma_s \tau - \gamma_\infty \tau_s} e^{-t/\tau}\right]. \tag{16c}$$

After combining $D_1(t)$ and $D_2(t)$ into a single time-dependent diffusion coefficient $D(t)$, where $D(t) \equiv D_1(t) + D_2(t)$, Eq. (16a) simplifies to

$$\frac{\partial P(\mathbf{x}, t)}{\partial t} = D(t) \nabla_{\mathbf{x}}^2 P(\mathbf{x}, t), \tag{17}$$

which is the starting point for the subsequent calculations.

IV. SURVIVAL PROBABILITY AND FIRST-PASSAGE DISTRIBUTION

As the next step in describing particle motion in a sphere, the diffusion equation of Eq. (17) is transformed from rectangular coordinates x_1, x_2, x_3 to spherical polar coordinates r, θ, ϕ; this leads to [50]

$$\left(\frac{\partial}{\partial t} - D(t)\left\{\frac{\partial^2}{\partial r^2} + \frac{2}{r}\frac{\partial}{\partial r} + \frac{1}{r^2 \sin\theta}\frac{\partial}{\partial \theta}\sin\theta\frac{\partial}{\partial \theta} + \frac{1}{r^2 \sin^2\theta}\frac{\partial^2}{\partial \phi^2}\right\}\right) P = 0, \tag{18}$$

where $P = P(r, \theta, \phi, t)$. After the change of variables $\mu = \cos\theta$ and $F = \sqrt{r}P$, Eq. (18) becomes

$$\left(\frac{\partial}{\partial t} - D(t)\left\{\frac{\partial^2}{\partial r^2} + \frac{1}{r}\frac{\partial}{\partial r} - \frac{1}{4r^2} + \frac{1}{r^2}\frac{\partial}{\partial \mu}(1 - \mu^2)\frac{\partial}{\partial \mu} + \frac{1}{r^2(1 - \mu^2)}\frac{\partial^2}{\partial \phi^2}\right\}\right) F = 0, \tag{19}$$

with $F = F(r, \mu, \phi, t)$. As shown in the Appendix, Eq. (19) can be solved by the method of separation of variables [51]. The solution, on imposing the condition that P vanish at the surface of the sphere located at $r = L$, takes the form

$$P(r, \mu, \phi, t) = \frac{1}{\sqrt{r}} \sum_{l,m,n} A_{lmn} e^{im\phi} J_{n+1/2}(y_{nl} r/L) P_n^m(\mu) \exp\left[-\frac{y_{nl}^2}{L^2}\int_0^t dt' D(t')\right]. \tag{20}$$

Here A_{lmn} is an as yet unknown expansion coefficient, $J_\nu(x)$ is a Bessel function of order ν, y_{nl} is the lth root of $J_{n+1/2}(x)$, i.e., $J_{n+1/2}(y_{nl}) = 0$, with $l = 1, 2, \ldots$, and $P_n^m(\mu)$ is an associated Legendre function. The coefficient A_{lmn} is now obtained by applying the initial condition $P(r, \mu, \phi, 0) = r^{-2}\delta(r - r_0)\delta(\mu - \mu_0)\delta(\phi - \phi_0)$ to Eq. (20), multiplying the result by $r^{3/2} e^{-im'\phi} J_{n'+1/2}(y_{n'l'} r/L) P_{n'}^{m'}(\mu)$, and integrating over ϕ, μ, and r, from, respectively, 0 to 2π, -1 to $+1$, and 0 to L. The orthogonality relations

$$\int_0^{2\pi} d\phi e^{i\phi(m - m')} = 2\pi \delta_{m,m'}$$

and

$$\int_{-1}^{1} d\mu P_n^{m'}(\mu) P_{n'}^{m'}(\mu) = \frac{2}{2n + 1}\frac{(n + m')!}{(n - m')!}\delta_{n,n'}$$

as well as the following equation (which is obtained from the application of the boundary condition to various Bessel identities [52]),

$$\int_0^L dr r J_{n'+1/2}(y_{n'l} r/L) J_{n'+1/2}(y_{n'l'} r/L) = \frac{1}{2} L^2 J_{n'-1/2}^2(y_{n'l}) \delta_{l,l'}$$

then allow A_{lmn} to be determined in closed form. With A_{lmn} in hand, the distribution function is finally found to be

$$P(r, \mu, \phi, t) = \frac{(2\pi L^2)^{-1}}{\sqrt{r r_0}} \sum_{lmn} \frac{(n - m)!}{(n + m)!}\frac{(2n + 1)}{J_{n-1/2}^2(y_{nl})} e^{im(\phi - \phi_0)} J_{n+\frac{1}{2}}\left(\frac{y_{nl} r}{L}\right) J_{n+\frac{1}{2}}\left(\frac{y_{nl} r_0}{L}\right) \times P_n^m(\mu) P_n^m(\mu_0) \exp\left[-\frac{y_{nl}^2}{L^2}\int_0^t dt' D(t')\right]. \tag{21}$$

From this expression, the survival probability $S(t|r_0, \mu_0, \phi_0)$ that the particle remains in the interval between 0 and L up to time t after having started from the point r_0, μ_0, ϕ_0 can be determined as

$$S(t|r_0, \mu_0, \phi_0) = \int_0^L dr \int_{-1}^{1} d\mu \int_0^{2\pi} d\phi r^2 \, P(r, \mu, \phi, t). \tag{22}$$

When Eq. (21) for $P(r,\mu,\phi,t)$ is substituted into Eq. (22), and the integrals over, first ϕ, and then μ, are carried out, using the results $\int_0^{2\pi} d\phi e^{im\phi} = 2\pi\delta_{m,0}$, $P_n^0(\mu) = P_n(\mu)$, where $P_n(\mu)$ is a Legendre polynomial, $\int_{-1}^{1} d\mu P_n(\mu) = 2\delta_{n,0}$, and $P_0(\mu_0) = 1$, the expression for the survival probability reduces to

$$S(t|r_0,\mu_0,\phi_0) = \frac{2}{L^2}\sum_l \frac{J_{1/2}(y_{0l}r_0/L)}{\sqrt{r_0}J_{-1/2}^2(y_{0l})}\int_0^L dr r^{3/2}J_{1/2}(y_{0l}r/L)\exp\left[-\frac{y_{0l}^2}{L^2}\int_0^t dt' D(t')\right]. \tag{23}$$

The integral over r in Eq. (23) can now be obtained in closed form as [52]

$$\int_0^L dr r^{3/2}J_{1/2}(y_{0l}r/L) = \sqrt{\frac{2}{\pi}}\left(\frac{L}{y_{0l}}\right)^{5/2}[-y_{0l}\cos y_{0l} + \sin y_{0l}]. \tag{24}$$

From its definition, y_{0l} is the solution to the equation $J_{1/2}(y_{0l}) = 0$, and since $J_{1/2}(z) = \sqrt{2/(\pi z)}\sin z$, it follows that $y_{0l} = l\pi$, $l = 1, 2, \ldots$, and therefore

$$\int_0^L dr r^{3/2}J_{1/2}(y_{0l}r/L) = \sqrt{\frac{2}{\pi}}\left(\frac{L}{l\pi}\right)^{5/2}[-l\pi(-1)^l]. \tag{25}$$

If it is now assumed (for convenience) that the particle is initially located at $r_0 = 0$, then the result $\lim_{r_0\to 0} J_{1/2}(y_{0l}r_0/L)/\sqrt{r_0} = \sqrt{2l/L}$ along with the result $J_{-1/2}(y_{0l}) = (-1)^l\sqrt{2/(\pi^2 l)}$, leads to

$$S(t|0) = 2\sum_l (-1)^{l+1}\exp\left[-\frac{l^2\pi^2}{L^2}\int_0^t dt' D(t')\right]. \tag{26}$$

The sum in this expression can be evaluated analytically [52]; the result is

$$S(t|0) = 1 - \vartheta_4(0, e^{-g(t)}), \tag{27}$$

where $g(t) = (\pi^2/L^2)\int_0^t dt' D(t')$ and $\vartheta_4(0,z)$ is an elliptic theta function (specifically Jacobi's fourth theta function), defined as $\vartheta_4(u,q) = 1 + 2\sum_{n=1}^{\infty}(-1)^n q^{n^2}\cos 2nu$.

The first-passage distribution, $f(t)$, is now obtained from the relation [40]

$$f(t) = -\frac{\partial S(t|0)}{\partial t}. \tag{28}$$

Once $g(t)$ is specified, both $S(t|0)$ and $f(t)$ can be calculated as functions of t and the other parameters defining the system. From the definitions of $D_1(t)$ and $D_2(t)$ in Eqs. (16b) and (16c), $g(t)$ is readily found to be

$$g(t) = \frac{\pi^2 k_B T}{\gamma_s L^2}\left[t + \frac{\tau_s(\gamma_s-\gamma_\infty)}{\gamma_s}(1-e^{-B_1 t})\right] + \frac{\pi^2\tau\varepsilon}{\gamma_s^2 L^2}\left[t + \frac{1}{B_1}(A_1+A_2)(1-e^{-B_1 t}) + \frac{A_1A_2}{2B_1}(1-e^{-2B_1 t})\right.$$
$$\left. - \frac{A_1A_3\tau}{(1+\tau B_1)}(1-e^{-B_1 t - t/\tau}) - \tau A_3(1-e^{-t/\tau})\right], \tag{29a}$$

where $A_1 = (\gamma_s-\gamma_\infty)/\gamma_\infty$, $A_2 = \tau_s(\gamma_\infty-\gamma_s)/(\gamma_s\tau - \gamma_\infty\tau_s)$, $A_3 = \gamma_s(\tau-\tau_s)/(\gamma_s\tau - \gamma_\infty\tau_s)$, and $B_1 = \gamma_s/(\gamma_\infty\tau_s)$.

To highlight the effects of self-propulsion and viscoelasticity on $S(t|0)$ and $f(t)$ it proves helpful, as a first step, to introduce a characteristic time scale t_0 that is a measure of the time taken by the particle, on average, to reach the boundary of the cavity under *passive* diffusion. This time scale can be taken as $t_0 = L^2/D$ [42], where D is the diffusion coefficient, which is given by $D = k_B T/\gamma_s$. The amplitude of the driving force, ε, determines the particle's speed of self-propulsion v, the two being related as $\varepsilon = v^2\gamma_s^2/3$ [15]. The dimensionless combination vt_0/L is then effectively the ratio of active to passive diffusion, and can be identified with the Péclet number Pe [42]. In terms of this number and the scaled times $\bar{t} \equiv t/t_0$ and $\bar{\tau} \equiv \tau/t_0$, the function $g(t)$ assumes the form

$$g(\bar{t}) = \pi^2\bar{t}\left[1 + \frac{\tau_s(\gamma_s-\gamma_\infty)}{\bar{t}\,t_0\gamma_s}(1-e^{-B_1 t_0\bar{t}})\right] + \frac{\pi^2\mathrm{Pe}^2\bar{\tau}\bar{t}}{3}\left[1 + \frac{1}{B_1\bar{t}\,t_0}(A_1+A_2)(1-e^{-B_1 t_0\bar{t}}) + \frac{A_1A_2}{2B_1\bar{t}\,t_0}(1-e^{-2B_1 t_0\bar{t}})\right.$$
$$\left. - \frac{A_1A_3\bar{\tau}}{\bar{t}(1+B_1 t_0\bar{\tau})}(1-e^{-B_1 t_0\bar{t} - \bar{t}/\bar{\tau}}) - \frac{A_3\bar{\tau}}{\bar{t}}(1-e^{-\bar{t}/\bar{\tau}})\right]. \tag{29b}$$

The contribution of viscoelasticity to active particle dynamics can be gauged by calculating $S(t|0)$ and $f(t)$ for the case of a Markovian (memoryless) fluid, for which $K(t)$ in Eq. (1) is given simply by $2\delta(t)$. The only effect of changing $K(t)$ to this form is to modify the function $g(t)$, which, by passing to the limit $\tau_s \to \infty$ [cf. Eq. (15)] in Eq. (29), can be shown—in terms of scaled variables—to be given by

$$g(\bar{t}) = \frac{\pi^2\bar{t}\gamma_s}{\gamma_\infty}\left[1 + \frac{\mathrm{Pe}^2\gamma_s\bar{\tau}}{3\gamma_\infty}\left\{1 - \frac{\bar{\tau}}{\bar{t}}(1-e^{-\bar{t}/\bar{\tau}})\right\}\right]. \tag{30}$$

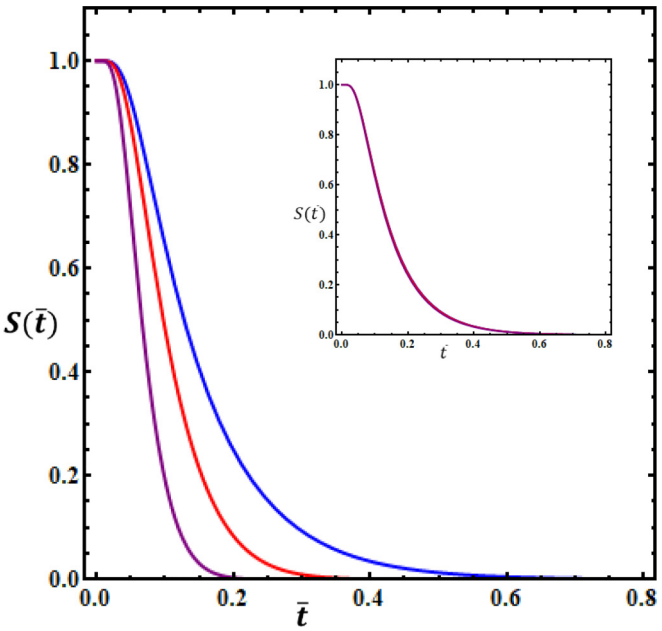

FIG. 1. The survival probability $S(\bar{t}|0)$ versus the scaled time $\bar{t}$ for a viscoelastic liquid, as calculated from Eqs. (27) and (29b), at fixed $\bar{\tau} = 1.0$ and at the following values of the Péclet number Pe: 0 (blue curve), 4.0 (red), and 8.0 (purple). Inset. $S(\bar{t}|0)$ versus time $\bar{t}$ for the same liquid at $\bar{\tau} = 0.001$ and at the same Pe (and color-coded) values as the main figure.

Equations (27) and (28) [along with Eqs. (29b) and (30)] are the main result of this paper. For both simple and complex liquids, they express the dependence of $S(t|0)$ and $f(t)$ on essentially just two parameters: the Péclet number Pe, which characterizes the strength of the self-propulsive forces, and the dimensionless relaxation time $\bar{\tau}$, which characterizes (as a fraction of the diffusion time t_0) the interval over which these forces can be said to persist. $S(t|0)$ and $f(t)$ also depend on the friction coefficients and relaxation time of the fluid, viz., γ_s, γ_∞, and τ_s, but these parameters do not change for a given fluid under specified conditions. (In the present case they apply specifically to an equimolar solution of cetylpyridinium chloride and sodium salicylate at 5 mM in deionized water [47].)

After assigning values to Pe and $\bar{\tau}$ (and to γ_s, γ_∞, τ_s, T, and L) in $g(\bar{t})$ in Eqs. (29) or (30), $S(t|0)$ is calculated from Eq. (27) and $f(t)$ from Eq. (28) using *Mathematica* [52]. The values assigned to γ_s, γ_∞, and τ_s are those shown in the paragraph following Eq. (15), while the temperature T is set to 300 K and the radius of the cavity L is set to the arbitrary (and freely adjustable) value of 1 μm (which is about the size of at least some eukaryotic cells). The values of γ_s, γ_∞, τ_s, T, and L are kept fixed throughout the calculations.

V. RESULTS AND DISCUSSION

The results of these calculations are summarized in Figs. 1–4, which highlight different aspects of the motion of spherically confined self-propelled particles.

Figure 1 shows plots of $S(\bar{t}|0)$ versus $\bar{t}$, as calculated from Eqs. (27) and (29b), at three different values of Pe (0, 4, and 8, corresponding, respectively, to the blue, red, and purple curves) and at the fixed value $\bar{\tau} = 1.0$. The values chosen for Pe are the same as those used in Ref. [42], and the decay curves of the survival probability at these values exactly mirror the decay curves in Fig. 4 of that reference. Each starts from 1.0 at $t = 0$ (when the survival of the particle is guaranteed), and decays to 0 at long times (when particle capture at the boundary becomes inevitable). The decay to 0 is fastest at the largest Péclet number (Pe = 8), and slowest at the smallest (Pe = 0), with the decay for Pe = 4 lying between the two extremes. These trends are in accord with intuition: increasing Pe increases the speed of the particle's self-propulsion, making it more likely—in relation to passive diffusion—that the particle will encounter (and be stopped at) the boundary of the cavity in a given interval of time, and making it less likely that it will survive within the cavity.

The decay curves in Fig. 1 are also found (data not shown) to be largely independent of $\bar{\tau}$ when $\bar{\tau}$ is greater than 1 (meaning there is little qualitative or quantitative difference between two decay curves with the same Pe value but different $\bar{\tau}$ values, provided $\bar{\tau} \geqslant 1$). By definition, $\bar{\tau} = \tau/t_0$, so values of $\bar{\tau}$ greater than 1 correspond to persistence times of the athermal forces that exceed the time t_0 for the particle to reach the boundary under passive diffusion. In these circumstances, when Pe is fixed, increasing $\bar{\tau}$ (beyond unity) has little effect on the particle's survival probability at a given time, since at $\bar{\tau} = 1$, the distance covered by the particle in the interval t_0 for which its self-propulsion speed v persists already exceeds the distance L at which absorption occurs. But the situation is different when $\bar{\tau} < 1$, that is, when the persistence time of the athermal forces falls below t_0. In this regime, the decay curves at different Pe tend to approach the decay curve for Pe = 0, a circumstance illustrated in the inset to Fig. 1, where for $\bar{\tau} = 0.001$, the decay curves corresponding to Pe = 4 and 8 collapse onto the curve at Pe = 0. This behavior originates in the fact that as $\bar{\tau}$ tends to 0, the athermal forces increasingly approach delta correlation, acting effectively in that limit as the ordinary Gaussian white noise driving passive diffusion.

These trends are replicated for the case of a simple (Markovian) fluid, as shown in Fig. 2, but the decays of $S(\bar{t}|0)$ to 0—at the same three value of Pe used in Fig. 1 (viz., 0, 4, and 8)—occur significantly faster. Again, these curves are $\bar{\tau}$ independent when $\bar{\tau} > 1$ (data not shown) and approach the Pe = 0 curve when $\bar{\tau} < 1$, collapsing onto it (see the inset to Fig. 2) when $\bar{\tau} = 0.0001$ (or smaller). The differences between the survival probabilities in Figs. 1 and 2 (which are quantitative, not qualitative) highlight the pronounced slowing down effect that viscoelasticity has on the particle's motion.

Figure 3 shows plots of the first-passage distribution $t_0 f(\bar{t})$ versus $\bar{t}$ for a viscoelastic fluid, as calculated from Eqs. (28), (27), and (29b), at fixed $\bar{\tau} = 1$ and at the following values of Pe: 0, blue curve; 4.0, red curve; and 8.0, purple curve. In the absence of self-propulsion, the distribution of first-passage times to the boundary is seen to be broadly and asymmetrically distributed, reflecting the intrinsic randomness of the particle's motion through the sphere. Under the action of self-propulsive forces, this motion becomes less random and more directed, and the distributions correspondingly become narrower and more symmetric. These trends are largely replicated in the distributions calculated by Di Trapani *et al.* [42] (see

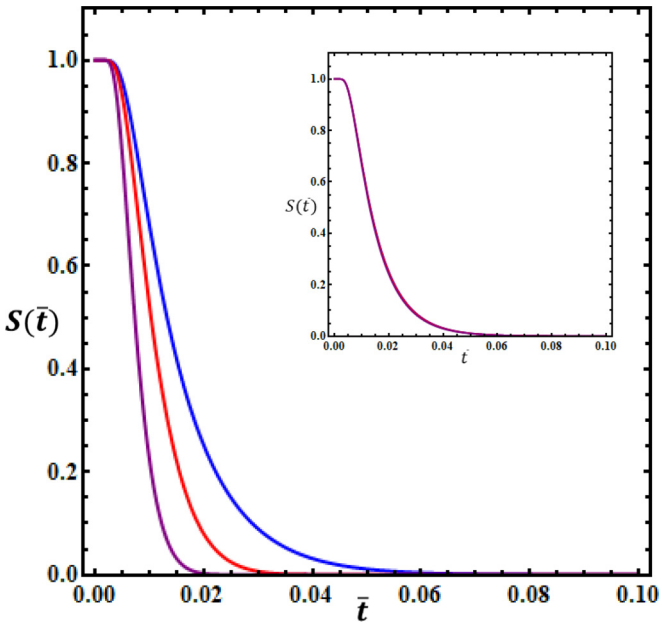

FIG. 2. The survival probability $S(\bar{t}|0)$ versus the scaled time $\bar{t}$ for a simple liquid, as calculated from Eqs. (27) and (30), at fixed $\bar{\tau} = 1.0$ and at the following values of the Péclet number Pe: 0 (blue curve), 4.0 (red), and 8.0 (purple). Inset. $S(\bar{t}|0)$ versus time $\bar{t}$ for the same liquid at $\bar{\tau} = 0.0001$ and at the same Pe (and color-coded) values as the main figure.

Fig. 5 in that reference), though the latter appear to display greater skewness overall.

Figure 4 shows plots of the first-passage distribution $t_0 f(\bar{t})$ versus $\bar{t}$ for a simple fluid, as calculated from Eqs. (28), (27),

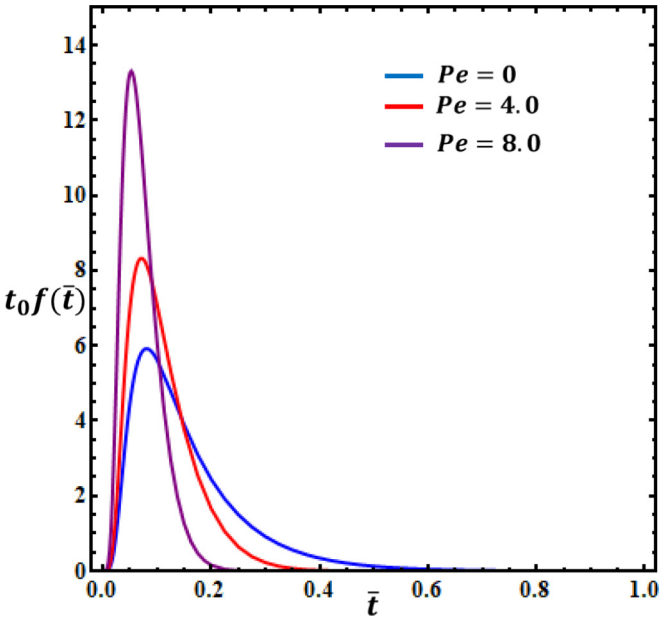

FIG. 3. The dimensionless waiting time distribution $t_0 f(\bar{t})$ versus the scaled time $\bar{t}$ for a viscoelastic liquid, as calculated from Eqs. (28), (27), and (29b), at fixed $\bar{\tau} = 1.0$ and at the following values of the Péclet number Pe: 0 (blue curve), 4.0 (red), and 8.0 (purple).

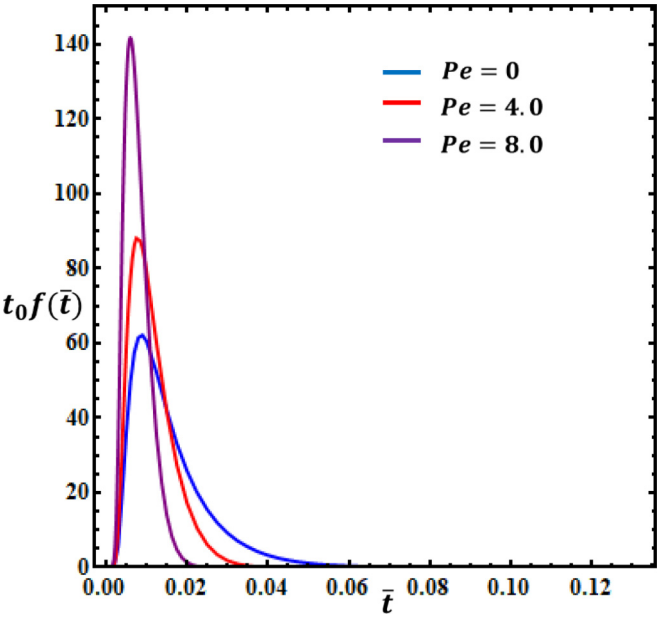

FIG. 4. The dimensionless waiting time distribution $t_0 f(\bar{t})$ versus the scaled time $\bar{t}$ for a simple liquid, as calculated from Eqs. (28), (27), and (30), at fixed $\bar{\tau} = 1.0$ and at the following values of the Péclet number Pe: 0 (blue curve), 4.0 (red), and 8.0 (purple).

and (30), at fixed $\bar{\tau} = 1$ and at the following values of Pe: 0, blue curve; 4.0, red curve; and 8.0, purple curve. Qualitatively, these curves are similar to the curves in Fig. 3, but they are all more narrowly distributed (even at Pe = 0), suggesting that viscoelastic effects may cause greater dispersion in the particle's trajectories, a possibility supported by the known occurrence of subdiffusion and other anomalous behaviors in the presence of such effects.

The findings presented here hint at the richness of the dynamical behavior that underlies autonomous motion under conditions of confinement. The model introduced in this paper, though simpler and perhaps less realistic [38,43] than the ABP model used in di Trapani *et al.*'s investigation [42], appears to capture much the same physics, and can therefore serve as a convenient, practical framework for exploring other aspects of confined active dynamics.

The data that support the findings of this study are available within the paper.

ACKNOWLEDGMENT

This work was supported by funds from the Indian Institute of Science, Bangalore, India.

The author has no conflicts of interest to disclose.

APPENDIX: DERIVATION OF EQ. (20)

To show that the probability density function $P(r, \mu, \phi, t)$ is given by Eq. (20) under absorbing boundary conditions at $r = L$, one must find the solution of Eq. (19) for the function $F = F(r, \mu, \phi, t)$. This is done by first assuming that F can be written as a product of functions that depend separately on the variables r, μ, ϕ, and t, in other words, as

$F = G(t)R(r)M(\mu)\Phi(\phi)$. When this assumed form of F is substituted into Eq. (19), the resulting equation—after suppressing the arguments of G, R, M, and Φ to save space—can be rearranged to

$$\frac{1}{D(t)G}\frac{\partial G}{\partial t} = \frac{1}{R}\left(\frac{\partial^2}{\partial r^2}+\frac{1}{r}\frac{\partial}{\partial r}-\frac{1}{4r^2}\right)R+\frac{1}{Mr^2}\frac{\partial}{\partial \mu}(1-\mu^2)\frac{\partial M}{\partial \mu} + \frac{1}{r^2(1-\mu^2)\Phi}\frac{\partial^2\Phi}{\partial\phi^2}. \tag{A1}$$

The left-hand side of this equation depends solely on t, while the right-hand side depends solely on r, μ, and ϕ, so it must follow that each side is a constant, independent of these variables, say, $-\lambda^2$. Hence,

$$\frac{1}{D(t)G}\frac{\partial G}{\partial t} = -\lambda^2 \tag{A2}$$

and

$$\frac{1}{R}\left(\frac{\partial^2}{\partial r^2}+\frac{1}{r}\frac{\partial}{\partial r}-\frac{1}{4r^2}\right)R+\frac{1}{Mr^2}\frac{\partial}{\partial \mu}(1-\mu^2)\frac{\partial M}{\partial \mu} + \frac{1}{r^2(1-\mu^2)\Phi}\frac{\partial^2\Phi}{\partial\phi^2} = -\lambda^2. \tag{A3}$$

Equation (A3), in turn, can be rearranged to

$$-\frac{1}{\Phi}\frac{\partial^2\Phi}{\partial\phi^2} = \frac{r^2(1-\mu^2)}{R}\left(\frac{\partial^2}{\partial r^2}+\frac{1}{r}\frac{\partial}{\partial r}-\frac{1}{4r^2}\right)R + \lambda^2 r^2(1-\mu^2)+\frac{(1-\mu^2)}{M}\frac{\partial}{\partial\mu}(1-\mu^2)\frac{\partial M}{\partial\mu}. \tag{A4}$$

Again, because the left-hand side of this equation is a function of ϕ alone, and the right-hand side is independent of it, each side must equal a constant, in this case, m^2, say. Accordingly,

$$\frac{1}{\Phi}\frac{\partial^2\Phi}{\partial\phi^2} = -m^2 \tag{A5}$$

and

$$\frac{r^2}{R}\left(\frac{\partial^2}{\partial r^2}+\frac{1}{r}\frac{\partial}{\partial r}-\frac{1}{4r^2}\right)R+\lambda^2 r^2 = \frac{m^2}{1-\mu^2}-\frac{1}{M}\frac{\partial}{\partial\mu}(1-\mu^2)\frac{\partial M}{\partial\mu}. \tag{A6}$$

The same reasoning applied to Eq. (A.6) now leads to two further equations:

$$\frac{\partial}{\partial\mu}(1-\mu^2)\frac{\partial M}{\partial\mu}+\left(n(n+1)-\frac{m^2}{1-\mu^2}\right)M = 0 \tag{A7}$$

and

$$\frac{1}{R}\left(\frac{\partial^2}{\partial r^2}+\frac{1}{r}\frac{\partial}{\partial r}-\frac{1}{4r^2}\right)R+\lambda^2 = \frac{n(n+1)}{r^2}, \tag{A8a}$$

or, equivalently,

$$\left(\frac{\partial^2}{\partial r^2}+\frac{1}{r}\frac{\partial}{\partial r}\right)R+\left(\lambda^2-\frac{(n+1/2)^2}{r^2}\right)R = 0, \tag{A8b}$$

Where n is another constant. Equations (A2), (A5), (A7), and (A8b) for the functions G, Φ, M, and R are readily solved, the solutions being $G(t) \propto \exp[-\lambda^2\int_0^t dt' D(t')]$, $\Phi(\phi) \propto e^{im\phi}$, $M(\mu) \propto P_n^m(\mu)$, and $R(r) \propto J_{n+1/2}(\lambda r)$, where $P_n^m(x)$ is an associated Legendre function, and $J_\alpha(x)$ is a Bessel function of index α.

The requirement that the surface of the sphere at $r = L$ be an absorbing boundary fixes the constant λ as y_{nl}/L, where y_{nl} is the lth zero of $J_{n+1/2}(z)$, i.e., it is the solution of the equation $J_{n+1/2}(y_{nl}) = 0$.

The foregoing results immediately identify Eq. (20) as the most general form of the probability density function $P(r, \mu, \phi, t)$ satisfying the given boundary conditions.

[1] R. Phillips, J. Kondev, J. Theriot, and H. G. Garcia, *Physical Biology of the Cell*, 2nd ed. (Garland Science, Taylor & Francis LLC, New York, 2013).

[2] G. Seisenberger, M. U. Ried, T. Endress, H. Büning, M. Hallek, and C. Bräuchle, Real-time single-molecule imaging of the infection pathway of an adeno-associated virus, Science **294**, 1929 (2001).

[3] U. F. Greber and M. Way, A superhighway to virus infection, Cell **124**, 741 (2006).

[4] N. Arhel, A. Genovesio, K.-A. Kim, S. Miko, E. Perret, J.-C. Olivo-Marin, S. Shorte, and P. Charneau, Quantitative four-dimensional tracking of cytoplasmic and nuclear HIV-1 complexes, Nat. Methods **3**, 817 (2006).

[5] E.-M. Damm and L. Pelkmans, Systems biology of virus entry in mammalian cells, Cell. Microbiol. **8**, 1219 (2006).

[6] X.-L. Wu and A. Libchaber, Particle diffusion in a quasi-two-dimensional bacterial bath, Phys. Rev. Lett. **84**, 3017 (2000).

[7] X. Zheng, B. ten Hagen, A. Kaiser, M. Wu, H. Cui, Z. Silber-Li, and H. Löwen, Non-Gaussian statistics for the motion of self-propelled Janus particles: Experiment vs theory, Phys. Rev. E **88**, 032304 (2013).

[8] J. R. Gomez-Solano and C. Bechinger, Transient dynamics of a colloidal particle driven through a viscoelastic fluid, New J. Phys. **17**, 103032 (2015).

[9] J. Elgeti, R. G. Winkler, and G. Gompper, Physics of microswimmers – single particle motion and collective behavior: A review, Rep. Prog. Phys. **78**, 056601 (2015), and references therein.

[10] J. R. Gomez-Solano, A. Blokhuis, and C. Bechinger, Dynamics of self-propelled Janus particles in viscoelastic fluids, Phys. Rev. Lett. **116**, 138301 (2016).

[11] C. Lozano, J. R. Gomez-Solano, and C. Bechinger, Run-and-tumble-like motion of active colloids in viscoelastic media, New J. Phys. **20**, 015008 (2018).
[12] J. C. Aragones, S. Yazdi, and A. Alexander-Katz, Diffusion of self-propelled particles in complex media, Phys. Rev. Fluids **3**, 083301 (2018).
[13] H. Löwen, Inertial effects of self-propelled particles: From active Brownian to active Langevin motion, J. Chem. Phys. **152**, 040901 (2020).
[14] O. Chepizko and T. Franosch, Random motion of a circle microswimmer in a random environment, New J. Phys. **22**, 073022 (2020).
[15] Y. Kim, S. Joo, W. K. Kim, and J.-H. Jeon, Active diffusion of self-propelled particles in flexible polymer networks, Macromolecules **55**, 7136 (2022).
[16] L. Piro, B. Mahault, and R. Golestanian, Optimal navigation of microswimmers in complex and noisy environments, New J. Phys. **24**, 093037 (2022).
[17] R. Sahoo, L. Theeyancheri, and R. Chakrabarti, Transport of a self-propelled tracer through a hairy cylindrical channel: Interplay of stickiness and activity, Soft Matter **18**, 1310 (2022).
[18] R. S. Yadav, C. Das, and R. Chakrabarti, Dynamics of a spherical self-propelled tracer in a polymeric medium: Interplay of self-propulsion, stickiness, and crowding, Soft Matter **19**, 689 (2023).
[19] A. Ajdari, Transport by active filaments, Europhys. Lett. **31**, 69 (1995).
[20] T. Bickel, A note on confined diffusion, Phys. A (Amsterdam, Neth.) **377**, 24 (2007).
[21] T. Lagache and D. Holcman, Quantifying intermittent transport in cell cytoplasm, Phys. Rev. E **77**, 030901(R) (2008).
[22] C. P. Brangwynne, G. H. Koenderink, F. C. MacKintosh, and D. A. Weitz, Intracellular transport by active diffusion, Trends Cell Biol. **19**, 423 (2009).
[23] P. Hänggi and F. Marchesoni, Artificial Brownian motors: Controlling transport on the nanoscale, Rev. Mod. Phys. **81**, 387 (2009).
[24] D. A. Kenwright, A. W. Harrison, T. A. Waigh, P. G. Woodman, and V. J. Allan, First-passage-probability analysis of active transport in live cells, Phys. Rev. E **86**, 031910 (2012).
[25] P. C. Bressloff and J. M. Newby, Stochastic models of intracellular transport, Rev. Mod. Phys. **85**, 135 (2013).
[26] G. Szamel, 2014 Self-propelled particle in an external potential: Existence of an effective temperature, Phys. Rev. E **90**, 012111 (2014).
[27] S. Das, G. Gompper, and R. G. Winkler, Confined active Brownian particles: Theoretical description of propulsion induced accumulation, New J. Phys. **20**, 015001 (2018).
[28] S. Song, A. Llopis-Lorente, A. F. Mason, L. K. E. A. Abdelmohsen, and J. C. M. van Hest, Confined motion: Motility of active microparticles in cell-sized lipid vesicles, J. Am. Chem. Soc. **144**, 13831 (2022).
[29] Z. Schuss, A. Singer, and D. Holcman, The narrow escape problem for diffusion in cellular microdomains, Proc. Natl. Acad. Sci. USA **104**, 16098 (2007).
[30] P. K. Ghosh, Escape kinetics of self-propelled Janus particles from a cavity: Numerical simulations, J. Chem. Phys. **141**, 061102 (2014).
[31] D. Holcman and Z. Schuss, *Stochastic Narrow Escape in Molecular and Cellular Biology* (Springer, New York, 2015).
[32] A. Geiseler, P. Hänggi, and G. Schmid, Kramers escape of a self-propelled particle, Eur. Phys. J. B **89**, 175 (2016).
[33] M. Paoluzzi, L. Angelani, and A. Puglisi, Narrow-escape time and sorting of active particles in circular domains, Phys. Rev. E **102**, 042617 (2020).
[34] T. Debnath, P. Chaudhury, T. Mukherjee, D. Mondal, and P. K. Ghosh, Escape kinetics of self-propelled particles from a circular cavity, J. Chem. Phys. **155**, 194102 (2021).
[35] P. C. Bressloff, Stochastically switching diffusion with partially reactive surfaces, Phys. Rev. E **106**, 034108 (2022).
[36] P. C. Bressloff, Diffusion-mediated absorption by partially-reactive targets: Brownian functionals and generalized propagators, J. Phys. A **55**, 205001 (2022).
[37] K. J. Modica, A. K. Omar, and S. C. Takatori, Boundary design regulates the diffusion of active matter in heterogeneous environments, Soft Matter **19**, 1890 (2023).
[38] L. Caprini, U. M. B. Marconi, A. Puglisi, and A. Vulpiani, Active escape dynamics: The effect of persistence on barrier crossing, J. Chem. Phys. **150**, 024902 (2019).
[39] R. Zwanzig, *Nonequilibrium Statistical Mechanics* (Oxford University Press, New York, 2001).
[40] C. W. Gardiner, *Handbook of Stochastic Methods for Physics, Chemistry and the Natural Sciences*, 3rd ed. (Springer-Verlag, Berlin, 2004).
[41] S. Iyer-Biswas and A. Zilman, First passage processes in cellular biology, Adv. Chem. Phys. **160**, 261 (2016).
[42] F. Di Trapani, T. Franosch, and M. Caraglio, Active Brownian particles in a circular disk with an absorbing boundary, Phys. Rev. E **107**, 064123 (2023).
[43] L. Caprini, E. Hernández-Garcia, C. López, and U. M. B. Marconi, A comparative study between two models of active cluster crystals, Sci. Rep. **9**, 16687 (2019).
[44] S. Okuyama and D. Oxtoby, The generalized Smoluchowski equation and non-Markovian dynamics, J. Chem. Phys. **84**, 5824 (1986).
[45] S. Chaudhury and B. J. Cherayil, Complex chemical kinetics in single enzyme molecules: Kramers' model with fractional Gaussian noise, J. Chem. Phys. **125**, 024904 (2006).
[46] E. A. Novikov, Functionals and the random force method in turbulence theory, Sov. Phys. JETP **20**, 1290 (1965).
[47] B. R. Ferrer, J. R. Gomez-Solano, and A. V. Arzola, Fluid viscoelasticity triggers fast transitions of a Brownian particle in a double well optical potential, Phys. Rev. Lett. **126**, 108001 (2021).
[48] F. Ginot, J. Caspers, M. Krüger, and C. Bechinger, Barrier crossing in a viscoelastic bath, Phys. Rev. Lett. **128**, 028001 (2022).
[49] B. J. Cherayil, Particle dynamics in viscoelastic media: Effects of non-thermal white noise on barrier crossing rates, J. Chem. Phys. **155**, 244903 (2021).
[50] P. Bhattacharyya, R. Sharma, and B. J. Cherayil, Confinement and viscoelastic effects on chain closure dynamics, J. Chem. Phys. **136**, 234903 (2012).
[51] M. N. Özişik, *Heat Conduction*, 2nd ed. (John Wiley & Sons, Inc., New York, 1993).
[52] Wolfram Research, Inc. *Mathematica*, Version 9.0 (Champaign, IL, 2012).